

Air-sea interaction and the seasonal cycle of the subtropical anticyclones*

Richard Seager¹, Ragu Murtugudde², Naomi Naik¹, Amy Clement³, Neil Gordon^{1†}
and Jennifer Miller¹

¹*Lamont-Doherty Earth Observatory of Columbia University*

Palisades, New York 10964

email: rich@maatkare.ldeo.columbia.edu

²*ESSIC, University of Maryland,*

College Park, Maryland.

³*Rosenstiel School of Marine and Atmospheric Sciences,*

University of Miami,

Miami, Florida.

Submitted to:

Journal of Climate

May 3, 2002

*Contribution number XXXX of Lamont Doherty Earth Observatory, copies available at <http://rainbow.ldeo.columbia.edu/jennie>

[†]Current affiliation: Scripps Institute for Oceanography, University of California at San Diego, La Jolla, California

Abstract

The causes of the seasonal cycles of the subtropical anticyclones, and the associated zonal asymmetries of sea surface temperature (SST) across the subtropical oceans, are examined. In all basins the cool waters in the east and warm waters in the west are sustained by a mix of atmosphere and ocean processes. When the anticyclones are best developed, during local summer, subsidence and equatorward advection on the eastern flanks of the anticyclones cool SSTs, while poleward flow on the western flanks warms SSTs. During local winter the SST asymmetry across the subtropical North Atlantic and North Pacific is maintained by warm water advection in the western boundary currents which offsets the large extraction of heat by advection of cold, dry air of the continents and by transient eddies. In the southern hemisphere ocean processes are equally important in cooling the eastern oceans by upwelling and advection during local winter. Although ocean dynamics are important in amplifying the SST asymmetry, experiments with general circulation models show that this amplification has little impact on the seasonal cycle of the anticyclones. Experiments with an idealized model are used to suggest that the subtropical anticyclones arise fundamentally as a response to monsoonal heating over land but need further amplification to bring them up to observed strength. The amplification is provided by local air-sea interaction. The SST asymmetry, generated through local air-sea interaction, by the weak anticyclones forced by heating over land stabilizes the atmosphere to deep convection in the east and destabilizes it in the west. Convection spreads from the land regions to the adjacent regions of the western subtropical oceans and the enhanced zonal asymmetry of atmospheric heating strengthens the subtropical anticyclones.

1. Introduction

In passing from Northern Hemisphere winter to summer the low level atmospheric circulation undergoes a dramatic transition. In Figure 1 we show seasonal maps of the sea level pressure and surface winds taken from National Centers For Environmental Prediction-National Center for Atmospheric Research (NCEP-NCAR) Reanalyses (Kalnay et al., 1996; Kistler and others, 2001). In Figure 2 we show seasonal maps of the precipitation Xie and Arkin (1996) and NCEP-NCAR Reanalysis subsidence at $700mb$. In the winter the Northern Hemisphere low level circulation is dominated by lows over the mid-latitude oceans while the subtropical anticyclones are weak and zonally elongated features. By early summer, precipitation is extensive over southeastern Asia and subtropical North America, the lows have almost disappeared and the subtropical anticyclones now occupy almost all of the northern hemisphere oceans. Strong meridional, equatorward, flow occurs on the eastern flank of the anticyclones and underlies strong subsidence. There is more diffuse southwesterly flow on the western flank and weak ascent. These arrangements are in accord with the prediction of Sverdrup balance $\beta v = f\omega_p$ where v is the meridional flow, ω is the vertical velocity in pressure p coordinates and β and f have their usual meaning (Rodwell and Hoskins 2001). Northeasterly trade wind flow on the southern flanks, and weak mid-latitude westerlies complete the circulation cells. As the seasonal transition occurs, the difference between the sea surface temperatures (SSTs) of the eastern and western subtropical oceans strengthens. This is also shown in Figure 1. In winter the eastern oceans are cooler than the west by only about $3^\circ C$ but in summer this difference grows to as much as $6^\circ C$. The cool waters in the east are reflected in lower surface air temperature and specific humidity resulting in strong moist static stability (Fig. 3) ensuring that convection will be shallow.

[Figure 1 about here.]

The seasonal cycle in the Southern Hemisphere has interesting similarities and differences with that in the north. In the Southern Hemisphere there is no large land mass and the subtropical surface pressure over the ocean maximizes at the end of winter when the Hadley Cell and mid-latitude westerlies are at their strongest. In the Northern Hemisphere maximum sea level pressure over the oceans occurs in summer due to the seasonal

exchange of mass between the Asian continent and the oceans caused by the massive Asian monsoon. However, as in the Northern Hemisphere, the Southern Hemisphere subtropical anticyclones are best developed as circulation cells (that is the departure from zonal symmetry is most pronounced) during the local spring and early summer season (September to January), similar to the Northern Hemisphere timing. At this time there is extensive precipitation over South America and Africa south of the equator (Fig. 2). In contrast, the zonal asymmetry of SST in the southern hemisphere is strongest during spring and actually weakens from spring to summer. These different seasonal cycles of SST and the subtropical anticyclones suggest that the balance of processes linking the oceans and the subtropical anticyclones must be different in the two hemispheres.

[Figure 2 about here.]

The seasonal cycle of SST asymmetry can be influenced by a number of processes. When the anticyclones are most developed, the eastern subtropical oceans experience equatorward flowing winds and subsidence, the western oceans poleward flowing winds and ascent. There is general equatorward flow in the ocean, and strong coastal upwelling, in the east and a poleward, westward intensified, boundary current in the west. There is also extensive boundary layer cloud cover (closely linked to the strong moist static stability shown in Fig. 3), which has a net cooling effect on climate (Hartmann et al., 1992; Klein and Hartmann, 1993), in the east but not in the west. Each of these processes could create the SST asymmetry but their relative contributions are not known. Further, each of them will tend to increase the asymmetry year round so what process weakens the asymmetry (i.e. cools the west relative to the east) as the anticyclones weaken?

The mechanisms that underlie the development and maintenance of the subtropical anticyclones are still in dispute. Rodwell and Hoskins (2001) suggest that the Pacific anticyclones develop as a remote response to summer convection over the Americas but also show that the Kelvin wave forced by heating in the Asian monsoon is important in forcing the equatorial, trade wind, part of both the North Pacific and North Atlantic anticyclones. Ting (1994) and Chen et al. (2001) have also argued that the northern anticyclones are forced by the Asian monsoon heating while heating in the region of the Americas (see Fig. 2 for example) simply breaks the high into two cells.

[Figure 3 about here.]

However, as Rodwell and Hoskins (2001) show, the anticyclones forced remotely by monsoonal heating are weak compared to observations. To bring them up to observed strength they appeal to 'diabatic amplification'. Forced descent creates a warm anomaly, enhanced radiative cooling and, therefore, enhanced descent which inhibits convection and latent heat release. However, NCEP-NCAR Reanalysis data show that the atmosphere is actually slightly cooler in the regions of descent than in the regions of ascent. The low levels of atmospheric moisture in the descent regions should also weaken the radiative cooling rates. However, Bergman and Hendon (2000) have shown that clouds reduce radiative cooling in regions of deep convection, and enhance radiative cooling in regions of shallow convection, and amplify the circulation forced by condensational heating providing an alternative mechanism for 'diabatic' amplification. In the current paper we examine whether local air-sea interactions, which lower the SST in regions of descent, and perhaps ocean dynamics as well, influence the development and maintenance of the subtropical anticyclones.

We will address the following questions:

- What atmospheric mechanisms influence the development of the zonal asymmetries of SST across the subtropical oceans and their seasonal cycle? Contenders are horizontal advection and subsidence by the mean flow, transient eddy fluxes and cloud radiative feedbacks, but what are the relative importance of these processes?
- How important is ocean heat transport in explaining the zonal asymmetry of SST and its seasonal cycle? Would the seasonal cycles of the subtropical anticyclones and their strength be different if the ocean heat transport was absent?
- To what extent can the subtropical anticyclones be understood as the remote response to monsoonal heating over land with the SST asymmetry arising as a response, or does the SST asymmetry subsequently impact the atmospheric circulation?
- Can air-sea interaction provide a mechanism whereby the atmospheric circulation, initially forced remotely by convective heating over land, creates zonal asymmetries of SST that favor precipitation over the western subtropical oceans which amplifies the initial circulation?

In Section 2 we describe the data sets and models used. Then, in Section 3, we present an observational analysis of the boundary layer moist static energy budget and surface radiation data to examine the atmospheric processes that can create the zonal asymmetries of SST. The remaining processes that determine the SST are ocean advection and mixing. These are derived from wind-forced simulations with ocean GCMs. This analysis will reveal the relative importance of mean horizontal advection of heat and moisture, mean subsidence warming and drying, transient eddy fluxes, cloud-radiation interactions and ocean heat transport in establishing the asymmetries of SST.

In Section 4, we turn to the simulation of the subtropical anticyclones and the zonal asymmetries of SST, and the mechanisms that force them, in two atmospheric GCMs coupled to mixed layer oceans. In one pair of experiments the mixed layer ocean contains a specified ‘q-flux’ which accounts for the ocean heat transport. In a second pair of experiments the q-flux is set to zero. In this case the influence of the ocean heat transport is removed. The GCM results suggest that the anticyclones are not greatly influenced by the ocean heat transport but that the SST asymmetry is. In Section 5 we describe experiments performed with an idealized atmosphere-ocean model that test this hypotheses. In Section 6 we propose a theory for the seasonal cycle of the subtropical anticyclones and associated zonal asymmetries of SST. Conclusions are offered in Section 7.

2. Observational data sets and models

a. Atmospheric data sets

The NCEP-NCAR Reanalysis data from 1949 to 2001 (Kalnay et al., 1996; Kistler and others, 2001) is used to derive estimates of the mean horizontal and vertical advection and the transient eddy divergence of moist static energy. Values of temperature, specific humidity, geopotential and zonal and meridional winds are used at levels from 700mb to 1000mb. The Reanalysis is also used for the sea level pressure and the SST. The Reanalysis cloud cover is poor, when compared to ship or satellite observations, over the eastern subtropical oceans. This primarily effects the surface solar radiation so for that we turn to satellite data but use NCEP-NCAR data for the surface longwave radiation.

b. Surface solar radiation

The surface solar radiation is taken from Earth Radiation Budget Experiment (ERBE) data (1985 to 1989) derived from satellite observations (Li and Leighton, 1993). Estimates of the surface solar from ERBE data are very similar to those from the independent (International Satellite Cloud Climatology Project (ISCCP) data (Bishop and Rossow, 1991), except for a simple offset (Seager and Blumenthal, 1994). Here we will only show results using the ERBE data.

c. Ocean GCMs

To derive estimates of the changes in SST due to ocean advection and mixing two wind-driven ocean GCMs are used. For the Northern Hemisphere we use the Lamont Ocean-Atmospheric Mixed Layer Model (LOAM). The model has been described by Visbeck et al. (1998). For the Pacific the configuration is described by Seager et al. (2001) and for the Atlantic by Seager et al. (2000). The model extends to $40^{\circ}S$ with meridional resolution varying from 0.5° near the equator to 2° in mid-latitudes and a fixed 2° resolution in longitude. Vertical resolution is concentrated in the upper 300m with fewer than 10 levels below. The model includes basin geometry and bathymetry consistent with the resolution. Temperature and salinity are restored to climatology at the southern boundary. The model includes a bulk wind-driven mixed layer model, convective adjustment and isopycnal thickness diffusion. In this model the mixed layer can contain several model levels.

LOAM performs poorly in the southeastern South Pacific. Instead, for both the South Pacific and the South Atlantic, we use the layer model of Murtugudde et al. (1996). This ocean GCM is a reduced gravity, primitive equation, sigma coordinate model (Gent and Cane, 1989) with an embedded hybrid mixing scheme (Chen et al., 1994). The vertical structure of the model ocean consists of a mixed layer and 19 layers below with the highest vertical resolution immediately below the mixed layer. The motionless deep layer is at $6^{\circ}C$ and 35 *psu* for the Atlantic and at $4^{\circ}C$ and 35 *psu* for the Pacific. The model domain for the Atlantic covers $40^{\circ}S$ - $40^{\circ}N$ and $45^{\circ}S$ - $65^{\circ}N$ for the Pacific. For both basins the meridional resolution is 0.5° but 0.33° in the $10^{\circ}S - 10^{\circ}N$ band and 0.66° in longitude.

Both ocean GCMs are coupled to the advective atmospheric mixed layer (AML) model

of Seager et al. (1995). The AML model computes the air temperature and air humidity together with the surface fluxes of latent and sensible heat and longwave radiation, using the modeled SST and the observed wind speed and direction. This methodology takes proper account of the thermodynamic coupling between the atmosphere and ocean that underlies how the SST is determined.

The ocean GCMs are forced by observed wind stresses, wind speeds and directions. For the North Pacific these are taken from daSilva et al. (1994), but elsewhere they are taken from NCEP-NCAR Reanalyses. The ocean GCMs also need the surface solar radiation which is taken from ERBE or ISCCP, corrected to remove the mean offset between them (see Seager and Blumenthal 1994).

d. Idealized atmosphere-ocean model

An idealized atmospheric GCM is used to model the atmospheric circulation variously forced by imposed heating over land and sea and its impact on the SST field. The dynamical core of the model is based on the Geophysical Fluid Dynamics Laboratory (GFDL) GCM. The model has rhomboidal truncation at zonal wavenumber 20 and 11 vertical layers. The circulation is forced by relaxation of the model temperature to the reference state of Held and Suarez (1994) plus specified heating. The vertical integral of the specified heating is equal to the latent heat released by condensation as estimated from the precipitation data of Xie and Arkin (1996). Dissipation is provided by a ∇^4 diffusion which damps the highest resolved wavenumber on a 2 day timescale. There is also a vertical momentum diffusion and friction in the lowest layer that damps with a 0.5 day timescale. The specific humidity is computed accounting for advection and using simple parameterizations of evaporation and rain out.

The atmosphere model forces a 50m deep mixed layer ocean model. The zonal mean SST in the mixed layer remains specified. Zonal deviations are computed in terms of the zonal deviation of the latent plus sensible heat flux (surface radiation is assumed to be zonally symmetric). The sensible and latent heat fluxes are computed by bulk formula. Deviations of SST from zonal symmetry in this model can only arise due to advection within the atmospheric circulation (mean plus transient) forced by imposed heating.

e. Climate models

Two different climate models were used. Each is an atmospheric GCM (AGCM) coupled to a mixed layer ocean. One AGCM is the Goddard Institute for Space Studies model (Hansen et al., 1984; Del Genio et al., 1996), a grid point model with $4^\circ \times 5^\circ$ resolution and 9 vertical levels. The other model is the National Center for Atmospheric Research (NCAR) Community Climate Model 3 (CCM3) (Kiehl et al., 1998) run with triangular truncation at zonal wavenumber 42 and 18 vertical levels. The GISS model is coupled to a mixed layer ocean whose depth varies in a specified way both seasonally and spatially (Russell et al., 1985) while the CCM3 is coupled to a mixed layer of uniform 50m depth. In each climate model the mixed layer contains a specified 'q-flux' constructed so that, when coupled, the model reproduces the observed SST with reasonable fidelity. The q-flux accounts for the movement of heat by the ocean as well as for errors in the model's surface heat fluxes. In companion experiments the q-flux was set to zero so that the SST was determined by a local balance of surface fluxes and SST tendency. The runs with a zero q-flux allow us to see the impact of the ocean heat transport on the seasonal cycle of subtropical SSTs and the subtropical anticyclones.

Both GCMs seriously underestimate boundary layer cloud cover over the eastern oceans. Their radiative impact on the SSTs is therefore included with the OHT in the specified q-flux. Setting the q-flux to zero therefore also removes the radiative impact of boundary layer clouds.

3. Observational analysis of subtropical air-sea interaction

a. Basic concepts and equations

The SST is determined by a balance of horizontal and vertical ocean advection, vertical ocean mixing and the net surface heat flux. On the atmospheric side the surface fluxes of heat, radiation and moisture are balanced by advection, subsidence, vertical mixing (or turbulence) and radiative fluxes. It is useful to combine the ocean and atmospheric boundary layers, by eliminating the surface fluxes, so we can examine the atmospheric

processes that create variations in SST. ¹

The SST equation can be written as:

$$\rho c_{pw} H \frac{\partial T}{\partial t} = OP - F_{solar}^0 - F_{LW}^0 - F_{SH}^0 - F_{LH}^0. \quad (1)$$

Here ρ is the density of water, c_{pw} is its specific heat, H is the mixed layer depth, T is the mixed layer temperature which equals the SST, OP is the SST tendency due to advection and mixing (see Appendix), and the F terms refer to the surface solar (F_{solar}^0) and longwave (F_{LW}^0) radiative fluxes, and the sensible (F_{SH}^0) and latent (F_{LH}^0) heat fluxes. The 0 superscript indicates a surface value. The surface flux terms are defined as positive upward but OP is defined as positive if it leads to an increase of SST.

The equation for the moist static energy, $h = c_p T_a + gz + Lq$, of the lower levels of the atmosphere, where T_a is the air temperature, z is the geopotential, q is the specific humidity and L is the latent heat of condensation, is given by:

$$\begin{aligned} \frac{1}{g} \int_{p_t}^{p_0} \left[\left(\frac{\bar{u}}{a \cos \phi} \frac{\partial \bar{h}}{\partial \lambda} + \frac{\bar{v}}{a} \frac{\partial \bar{h}}{\partial \phi} + \bar{\omega} \frac{\partial \bar{h}}{\partial p} \right) + \left(\frac{1}{a \cos \phi} \left(\frac{\partial (\overline{u'h'})}{\partial \lambda} + \frac{\partial (\overline{v'h'}) \cos \phi}{\partial \phi} \right) + \right. \\ \left. \frac{\partial (\overline{\omega'h'})}{\partial p} \right) \Big] dp = \int_{p_t}^{p_0} \left(\frac{\partial F_{RAD}}{\partial p} + \frac{\partial F_h}{\partial p} \right) dp \\ = F_{solar}^0 + F_{LW}^0 + F_{SH}^0 + F_{LH}^0 - F_{RAD}^{p_t} - F_h^{p_t}. \quad (2) \end{aligned}$$

Here c_p is the specific heat for air, λ is longitude, ϕ is latitude, F_{RAD} is the radiative flux, F_h is the turbulent flux of moist static energy, the overbars denote monthly means and primes denote departures from monthly means. $F_h^{p_t}$ is the turbulent flux of moist static energy at the top of the layer where the pressure is p_t and $F_{RAD}^{p_t}$ is the net radiative flux at this same level. The first bracketed term on the left within the square brackets is therefore the advection and subsidence of moist static energy by the mean flow and the second term is the transient eddy flux divergence of moist static energy.

By combining these two equations we derive an equation for the SST in terms of the

¹Looking at the surface fluxes alone can be misleading. For example the cool eastern subtropical oceans are places where the surface heat loss from the ocean is no larger than other longitudes at the same latitude. It might therefore be thought that atmospheric processes are not creating the cold SSTs but, instead, as atmospheric advection and subsidence cool the SST, and cloud cover reduces the incoming solar, the latent heat loss becomes less to restore a balance with close to zero net surface heat flux (Blumenthal, 1990).

ocean, atmosphere and radiative processes that alter it:

$$\rho c_{pw} H \frac{\partial T}{\partial t} = OP - \frac{1}{g} \int_{p_t}^{p_0} \left[\left(\frac{\bar{u}}{a \cos \phi} \frac{\partial \bar{h}}{\partial \lambda} + \frac{\bar{v}}{a} \frac{\partial \bar{h}}{\partial \phi} + \bar{\omega} \frac{\partial \bar{h}}{\partial p} \right) + \left(\frac{1}{a \cos \phi} \left(\frac{\partial (\overline{u'h'})}{\partial \lambda} + \frac{\partial (\overline{v'h'}) \cos \phi}{\partial \phi} \right) + \frac{\partial (\overline{\omega'h'})}{\partial p} \right) \right] dp - F_{RAD}^0 - \Delta N_T - F_h^{pt}. \quad (3)$$

where $\Delta N_T = F_{RAD}^{pt} - F_{RAD}^0$ is the radiative flux divergence across the atmospheric layer and is typically positive.

Of the terms on the right hand side, the SST tendency due to ocean processes (advection plus mixing), OP , will be evaluated from wind-forced ocean GCMs (see Appendix), the advection by the mean flow and the transient eddy flux divergence will be evaluated from NCEP-NCAR Reanalyses and the net radiation at the ocean surface, F_{RAD}^0 will be taken from ERBE for the solar component and NCEP-NCAR Reanalyses for the longwave component. Neither the radiative cooling of the lower levels of the atmosphere, ΔN_T , nor the convective mixing at the top of the level, F_h^{pt} , can be directly evaluated from the data. Here they are instead evaluated as a residual from Eq. 3. The SST itself is also taken from NCEP-NCAR Reanalyses.

b. Climatological air-sea interaction during summer and winter

Figure 4 shows the SST tendencies in DJF, in Wm^{-2} , due to each atmospheric or oceanic process. Figure 5 shows the same quantities for JJA.

[Figure 4 about here.]

[Figure 5 about here.]

In the subtropical northern hemisphere during winter the SST tendency due to mean advection and subsidence (Fig. 4a) cools the SST across the subtropical oceans. This reflects the zonally symmetric wintertime Hadley Cell. Outflow of cold, dry air from Asia and North America further cools the western oceans. In contrast, during summer (Fig. 5a) the mean circulation warms the western subtropical oceans and cools the eastern oceans. This reflects both the direction of horizontal flow around the subtropical anticyclones and

the localization of the descent in the east. In the east the vertical term is dominant and the subsidence warming part ($\approx 70Wm^{-2}$) is closely balanced by radiative cooling (Betts and Ridgway, 1989). The subsidence drying part is larger ($\approx 130Wm^{-2}$) and is balanced by evaporation, which cools the SST. The transient eddy moist static energy divergence (Figs. 4b and 5b) cools the subtropical SSTs throughout the year but by more in winter than summer and by more in the west than in the east.

The SST tendencies due to mean circulation and transients in the southern hemisphere have similar relationships to local season as in the northern hemisphere. The creation of the zonal asymmetry of SSTs by the mean flow is most obvious in local summer in the South Pacific (Fig. 4a). In the South Atlantic the mean circulation cools most in the central ocean. Transients cool both subtropical oceans throughout the year and by more in winter than summer, but the east to west difference in their effect is much smaller than in the north, due to the lack of marked continentality.

In the northern subtropics ocean processes (Figs. 4c and 5c) warm the west during winter and cool the east during summer. Both features are more confined to the coast than either the SST tendencies due to the atmospheric circulation or the basin scale features of the SST asymmetry itself. However, in the Southern Hemisphere, cooling by ocean processes extends considerably further west from the coast. The warming in the west is less strong than in the northern hemisphere, presumably due to the weaker western boundary currents.

The net solar radiation receipt by the ocean is quite zonally uniform during Northern Hemisphere winter. At other times, and in the Southern Hemisphere throughout the year, the eastern subtropical oceans get less radiation than areas to the west due to local maxima of low level cloud cover (Klein and Hartmann, 1993) but these features are confined near the coast.

c. Causes of the seasonal cycle of the asymmetry of SST across the subtropical oceans

In Figures 6 through 9 we plot the seasonal evolution of the SST and the terms on the right hand side of Eq. 3, that is the terms determining the SST, as a function of longitude. All quantities have been averaged over $15^\circ - 35^\circ N$ in the Northern Hemisphere and $25^\circ - 5^\circ S$ in the Southern Hemisphere. The southern latitude band is chosen to be closer to the

equator than the northern band to reflect the fact that the latitude of maximum SST asymmetry is also nearer the equator. All the terms are plotted as the departure from the zonal mean of the appropriate ocean basin. This allows us to look directly at the zonal asymmetry. Positive values indicate a warming tendency. Figure 6 is for the North Pacific, Figure 7 for the North Atlantic, Figure 8 for the South Pacific and Figure 9 for the South Atlantic.

i. The Northern Hemisphere In the North Pacific and North Atlantic the SST asymmetry (Figures 6a and 7a) has a maximum in August and a minimum in February. The seasonal cycle of the mean advection of moist static energy is the most obvious cause (Figures 6b and 7b): strong cooling in the east and warming in the west during April to July precedes the maximum of the SST asymmetry. Once the SST asymmetry has reached its full value the generation of the asymmetry by the mean advection has weakened. Shortly afterward, in the fall, the mean advection begins to cool the west of the Pacific Ocean but this effect is weak in the Atlantic. The winter mean advective cooling of the west is caused by the strengthening and southward shift of the mid-latitude westerlies and the advection of cold dry air off the continents. Transient eddies (Figures 6c and 7c) assist the winter cooling of the western oceans relative to the east. Consequently the atmospheric circulation, mean plus transient, creates the fundamentals of the seasonal cycle of the asymmetry of SST: mean advection strengthens the asymmetry from spring to summer and both the mean advection and transients weaken the asymmetry from fall through the winter. The wintertime weakening is almost strong enough that it would eliminate the SST asymmetry if it was unopposed.

The net surface radiation is shown in Figures 6d and 7d. Cloud-radiation interactions only have a modest impact on the seasonal cycle of the asymmetry and are particularly weak over the Atlantic Ocean where summertime cloud cover is less than over the North Pacific (Klein and Hartmann, 1993). The timing is consistent with the change in boundary layer clouds being a positive feedback: the atmospheric circulation creates cool SSTs in the east and increases the static stability (see Fig. 3) which, in turn, increases the boundary layer cloud cover causing further cooling of the SST. However this provides only a modest amplification of the SST asymmetry immediately west of the American and African coasts.

Cooling of the eastern oceans by advection and mixing in the ocean is also quite confined to the eastern coast (Figures 6e and 7e). More important is the large warming in the west during winter. This is primarily a result of the ocean mixed layer deepening, as it is cooled by strong surface heat loss sustained by cold, dry advection and transients, and entraining warmer waters from below. The temperatures of the waters below are themselves sustained by horizontal advection in the western boundary current. These ocean processes oppose the cooling by the mean and transient atmospheric circulation allowing the SST asymmetry to persist year round. In its absence we would expect the SST asymmetry to be much weaker.

[Figure 6 about here.]

[Figure 7 about here.]

The residual, the sum of radiative cooling of the boundary layer and the turbulent flux of moist static energy at its top (plus error), is shown in Figures 6f and 7f. We expect the boundary layer radiative cooling to be larger (on the order of $20Wm^{-2}$) in the west than in the east because of the greater water vapor content (Betts and Ridgway, 1989). This term contains the positive water vapor greenhouse feedback on the SST and will enhance the SST asymmetry by increasing the downward longwave flux in the west. However, the asymmetry of the turbulent flux at the top of the layer is probably larger. As the western oceans warm in summer deep convection occurs and fluxes moist static energy upward. In the east, convection is suppressed by the stable boundary layer. Hence the turbulent flux damps the SST asymmetry in the late summer season.

ii. The Southern Hemisphere In the southern hemisphere the SST asymmetry is strongest in October to December and weakest in March (Figs. 8a and 9a). Throughout the Southern Hemisphere winter the SST asymmetry is strengthening, in contrast to the Northern Hemisphere during winter when the asymmetry weakens. This difference seems to be a result of ocean processes playing a more important role in the southern hemisphere than the northern hemisphere. In both the South Pacific and the South Atlantic cooling by ocean processes (Figs. 8e and 9e) in the east is stronger than in the North and drives the strengthening of the SST asymmetry from March to October. Vertical entrainment of

cool water is the dominant term but the cool water is spread west by horizontal advection. Ocean dynamics are more important in explaining the SST asymmetry in the Southern Hemisphere than in the Northern Hemisphere for two reasons. First the winds blow parallel to the shore creating an ideal situation for coastal upwelling that is not matched in the North Pacific south of California (Philander et al., 1996). Second, the waters below the mixed layer are much cooler in the South Pacific and South Atlantic than in the North Pacific or North Atlantic (not shown), which, in turn, may in part be due to raising of the thermocline by the strong along shore flow but is also influenced by the proximity of the cold waters of the Southern Ocean.

In the South Pacific the mean advection of moist static energy (Figure 8b) strengthens the SST asymmetry most during local summer, as in the Northern Hemisphere. In the South Atlantic (Fig 9b) it tends to cool the central ocean relative to the areas to both the east and the west and with little variation through the year. This confirms ocean dynamics to be dominant in creating the observed SST asymmetry and its seasonal cycle in the southern hemisphere.

The impact of the transient eddy fluxes in both basins (Figs. 8c and 9c) is weak because the Southern Hemisphere stormtrack is far more zonally symmetric than its northern counterpart (which splits into two distinct centers east of the Asian and American coasts). Similar to the Northern Hemisphere subtropics, cloud-radiative feedbacks (Figs. 8d and 9d) provide an additional cooling of the SST in the east *after* the strong SST asymmetry has already been established. As in the northern hemisphere, the sum of radiative cooling of the boundary layer and the turbulent flux of moist static energy at its top (Figs 8f and 9f) damps the SST asymmetry.

[Figure 8 about here.]

[Figure 9 about here.]

4. Simulation of subtropical air-sea interaction with atmospheric GCMs coupled to mixed layer oceans

The previous analyses indicated that, while advection by the mean and transient atmospheric circulation is crucial to the generation of the zonal asymmetries of SST, OHT is

also important. In the northern hemisphere OHT maintains the asymmetry during winter and in the Southern Hemisphere cooling by OHT in the east is the dominant process creating the SST asymmetry.

Next we turn to a comparison of the subtropical anticyclones and asymmetry of SSTs as simulated by two pairs of atmospheric GCMs coupled to mixed layer oceans. In each pair one experiment accounts for the OHT in the mixed layer and the other experiment does not. On the basis of the observational analysis we expect that the SST asymmetry will be weaker than observed in the runs that do not account for OHT. However, the observational analysis cannot tell us what forces the seasonal cycle of the subtropical anticyclones. Here we examine whether weakening the zonal asymmetry of SSTs when the OHT is removed impacts the strength and seasonal cycle of the anticyclones.

The sea level pressure and deviation of SST from zonal symmetry for the two GISS models, for December through February and June through August, are shown in Figure 10 and the same results from the CCM3 model are shown in Figure 11. The models with the q-flux produce reasonable simulations of the seasonal cycle, strength and location of the subtropical anticyclones as can be seen by comparing Figures 10a and 10c and Figures 11a and 11c with Figure 1a and 1c.

[Figure 10 about here.]

[Figure 11 about here.]

Looking at the asymmetry of SST, it is clear that the basic patterns of warmer and colder than the zonal mean are reproduced in both models (and in mid-latitudes as well as in the tropics) but the asymmetry across the subtropical oceans is much weaker when the ocean heat transport is removed. When the ocean heat transport is removed the maximum SST asymmetry in the northern hemisphere still occurs in local summer but now it also occurs in local summer in the southern hemisphere. This supports the suggestion that ocean dynamics are the reason why the observed SST asymmetry in the southern hemisphere maximizes during local spring. The Northern Hemisphere subtropical anticyclones are not appreciably weaker when the ocean heat transport is removed. The Southern Hemisphere anticyclones do, however, appear to be weaker when the ocean heat transport is not accounted for. In both hemispheres the anticyclones are best defined in local summer whether or not the ocean heat transport is accounted for.

The GCMs have much less low level cloud cover over the eastern subtropical oceans than is observed and consequently underrepresent their cooling effect. This model deficiency helps explain why the SSTs are too warm in the far eastern subtropical basins but it is also clear that the clouds have little direct or indirect impact on the atmospheric circulation within these models.

The GCM results support the idea that ocean dynamics are required to achieve the strength of the observed subtropical SST asymmetry. Yet they also indicate that in the northern hemisphere the full asymmetry of the SST is not required for the subtropical anticyclones to achieve full strength while in the southern hemisphere it is. Since the precipitation over the tropical and subtropical oceans is closely related to SST, there are two possible explanations for these results. First, in the northern hemisphere, the subtropical anticyclones are forced largely by heating over land and are hardly altered when OHT is removed. Alternatively the subtropical anticyclones are forced by heating over both ocean and land but the weak SST asymmetry present when OHT is removed is enough to place the ocean precipitation in the correct location. In the southern hemisphere ocean heat transport is required to get both the SST asymmetry and the full strength of the subtropical anticyclones.

5. An idealized atmosphere-ocean model of subtropical air-sea interaction with imposed heating

The experiments with the atmospheric GCMs coupled to mixed layer oceans have made it clear that ocean heat transport is not essential in shaping the subtropical anticyclones. However local air-sea interactions may still influence the pattern of atmospheric heating that provides the forcing for the anticyclones. In this Section we will address the relative importance of the heating over the land and the sea. As in Rodwell and Hoskins (2001) we assume that the monsoon is 'triggered by land-sea sensible heating contrasts and is taken as given'. Here we use an idealized model to examine the circulation, and associated zonal asymmetry of SSTs, forced by monsoon heating over land alone. This will be compared to the circulation and SST asymmetry forced by heating over land and ocean. Then, by removing the ocean precipitation in the off-equatorial monsoon regions, we

will demonstrate how the atmospheric circulation forced by heating over land creates asymmetries of SST that favor convection over the western oceans which reinforces the original circulation.

The simple model of air-sea interaction contains an ocean mixed layer in which the SST is determined by surface fluxes alone, and an atmosphere model forced by imposed heating.

a. Atmosphere model

As described in Section 2 we use the dynamical core of the GFDL atmospheric GCM with an R20 truncation and 11 vertical layers. The temperature equation of the model is given by:

$$\frac{\partial T}{\partial t} + \mathbf{u} \cdot \nabla T + \omega \left(\frac{\partial T}{\partial p} - \frac{RT}{c_p p} \right) = Q - (T - T_R(y, p) + T_s^*) / \tau + D_T \quad (4)$$

where Q is the imposed heating due to condensation, $T_R(y, p)$, is a relaxation temperature that depends only on latitude and pressure derived using the observed zonal mean surface air temperature (from NCEP-NCAR Reanalysis) and the vertical profile from Held and Suarez (1994), T_s^* is the modeled deviation of the SST from zonal mean, τ is a timescale that varies between four days near the surface and 60 days at height and D is a horizontal and vertical diffusion. Hence the temperature is forced by the imposed heating and is relaxed to a zonal mean temperature adjusted by the modeled deviation of the surface temperature from the zonal mean. T_s^* is zero over land. In practice this feedback is very weak and the atmospheric circulation is essentially determined by the imposed heating. The vertical integral of the specified heating is equal to the latent heat released by condensation as estimated from the precipitation data of Xie and Arkin (1996). The heating is specified to peak in the mid-troposphere near the equator but at gradually lower levels with increasing distance from the equator. The imposed heating and T_R progress through a seasonal cycle linearly interpolating between monthly mean values.

The specific humidity, q , is computed from:

$$\frac{\partial q}{\partial t} + \mathbf{u} \cdot \nabla q + \omega \frac{\partial q}{\partial p} = E - M(q - q_{max}) / \tau_p + D_q. \quad (5)$$

Here $E = c_E U(q_s - q)/h$ is related to the surface evaporation and relaxes the specific humidity of the lowest model level (with depth h) to the surface saturation humidity, q_s , on a half day timescale. E is zero above the lowest model level. q_{max} is a maximum specific humidity above which moisture is removed on a quarter day timescale. q_{max} is taken to be 0.85 of its saturation value. To accomplish this, $M(q - q_{max})$ equals $q - q_{max}$ when $q - q_{max}$ is greater than zero and equals zero otherwise. D_q is a diffusivity. The specific humidity is therefore primarily influenced by horizontal advection and subsidence and impacts the evaporation and the modeled SST. However, it is important to remember that the condensational heating in the model remains specified and is not coupled to the modeled humidity distribution since our purpose is simply to examine how imposed heating can influence the temperature and humidity distribution over the ocean and, therefore, the SST.

b. Ocean mixed layer model

The seasonally varying zonal mean SST, $\langle T_s \rangle$, is specified from observations (NCEP-NCAR Reanalysis). The SST departure from zonal mean, T_s^* is determined from:

$$\frac{\partial T_s^*}{\partial t} = -\frac{\rho_a c_E}{\rho_w c_p H} [U(c_p \Delta T + L \Delta q) - \langle U(c_p \Delta T + L \Delta q) \rangle] \quad (6)$$

where U is the wind speed, H is the model ocean mixed layer depth (50m) and c_E is an exchange coefficient. ΔT and Δq are the air sea temperature and humidity differences given by:

$$\Delta T = T_s^* + \langle T_s \rangle - T, \quad (7)$$

$$\Delta q = q_s^* + \langle q_s \rangle - q. \quad (8)$$

q_s^* and $\langle q_s \rangle$ are the zonally asymmetric and zonally symmetric surface saturation humidity and T and q are the lowest level air temperature and specific humidity from the atmosphere model. Consequently, T_s^* is determined by the departure from the zonal mean of the surface latent plus sensible heat flux. Asymmetries of SST are driven by atmospheric motions which alter the air temperature and air humidity, modifying the surface fluxes and altering the SST until the departure from zonal mean of the latent plus sensible

surface flux returns to zero, satisfying Eq. 6.

[Figure 12 about here.]

[Figure 13 about here.]

c. Model results

The model is integrated for 10 years by which time the gross features are well established and steady.

In Figure 12 we show the sea level pressure and SST asymmetry during DJF forced by imposed heating over all land only (Fig. 12a, contour interval $2mb$), by imposed heating over all land plus the equatorial oceans between $15^{\circ}S$ and $15^{\circ}N$ (Fig 12b, contour interval $2mb$) and by imposed heating over all land plus all ocean (Fig 12c, contour interval $5mb$). The June through August simulations are shown in Figures 13. In the case with forcing over land only, during winter (Fig. 12a) the flow is quite zonal and in summer (Fig. 13a) the subtropical anticyclones are clearly present but weak (note the small contour interval). The asymmetries of the summer flow are enough to create cold waters over the eastern basins and warmer water over the western basins. The opposite sign asymmetry in the mid and high latitude North Atlantic is not recreated because of the lack of a developed Icelandic Low. When the essentially zonally symmetric (ITCZ) forcing in the equatorial region is added (Figs. 12b and 13b) the equatorial trough deepens but the flow becomes more zonal and the northern hemisphere subtropical anticyclones and SST asymmetry weaken.

The simulation of the sea level pressure and the SST asymmetry is quite realistic when all the forcing over both land and sea is included (Figs. 12c and 13c). In this case the North Pacific summer subtropical anticyclones achieves full strength but the Atlantic counterpart is misplaced. The quadropole pattern of the SST asymmetry, with opposite sign east-west asymmetries at subtropical and mid to high latitudes, is well recreated ². By comparing to the case that includes forcing over the ocean in only the equatorial region

²The mid to high latitude asymmetry arises as the winter Aleutian and Icelandic Lows achieve full development in response to orographic forcing and diabatic heating over the mid-latitude oceans (see Seager et al. (2002)).

(Figs. 11b and 12b), it is clear that the extensive condensational heating that occurs over the western subtropical oceans greatly strengthens the subtropical anticyclones.

The Southern Hemisphere simulation is poor. Neither the identity of the anticyclones nor the SST asymmetry are well reproduced. The ocean GCM demonstrated the importance of ocean heat transport so the poor simulation of the SST asymmetry is expected. However the simulation of the anticyclones is worse than in the atmospheric GCMs that also ignored the ocean heat transport indicating that the pattern of diabatic heating in the idealized model, imposed plus computed, is likely wrong. It is noteworthy that Rodwell and Hoskins (2001) were also unable to model the southern anticyclones unless they forced their model with the diabatic cooling (deduced from reanalyses) within the column immediately above.

6. A theory for the seasonal cycle of the subtropical anticyclones and associated zonal asymmetries of SST

Based on the analysis of observations and modeling so far reported, the following schematic can be presented for the seasonal cycle in the subtropics.

During winter the subtropical latitudes in each hemisphere are occupied by a zonal band of high pressure, underlying the subsiding branch of the Hadley Cell. During northern winter the ocean is cooled in the west by outflow of cold, dry air from the Asian and American continents. This cooling is opposed by poleward warm water advection within the western boundary currents ensuring maintenance of the SST asymmetry through the winter. As the transition to early summer occurs, convection over subtropical land areas begins and breaks the zonal symmetry of the atmospheric circulation. Vorticity balance requires poleward flow into the regions of deep convection while the part of the heating that is symmetric about the equator continues to force equatorial low pressure to the east via a Kelvin wave. Over the eastern oceans, where there is no deep convection, vorticity balance requires that radiatively driven descent be balanced by equatorward flow. In combination with weak mid-latitude westerlies this completes the formation of weak closed subtropical anticyclones. Air-sea interaction then comes into play to strengthen

the anticyclones.

Descent in the east causes subsidence drying and cools the SST while, in the west, poleward flow warms by horizontal advection. As a result, as the transition to summer occurs, the SST warms by more in the west than in the east. The atmosphere becomes very stable to deep convection in the east and unstable in the west allowing the spread of monsoonal convection over land to adjacent ocean regions. The extensive convection over the western subtropical oceans greatly enhances the forcing of the subtropical anticyclones. The SST asymmetry is then strengthened by the enhanced atmospheric circulation, and further enhanced by increased low cloud cover within the stable boundary layer in the east and by coastal upwelling. The vertical convective flux of moist static energy damps the SST asymmetry. Ultimately the subtropical anticyclones and the SST asymmetry weaken as summer ends and the precipitation, first over the subtropical land areas, and later over the subtropical oceans, weakens and finally shifts to the other hemisphere.

This better describes the northern hemisphere than the southern hemisphere. Cooling by ocean dynamics of the eastern oceans is important in the southern hemisphere but auxiliary in the north. During southern hemisphere winter, when the subtropical anticyclones are weak, strong southeasterly flow occurs along the coasts of South America and southern Africa as part of the winter Hadley Cell, causing strong upwelling and westward advection in the ocean and cooling. While the ocean heat transport is important in explaining the SST asymmetry it is less important in explaining the seasonal cycle of the southern subtropical anticyclones.

7. Conclusions

We have attempted to explain the seasonal cycle of the atmospheric circulation and the surface temperature of the ocean in the subtropics and assess the degree to which they arise as a coupled phenomena. The conclusions are as follows.

- In agreement with Rodwell and Hoskins (2001) the subtropical anticyclones owe their existence to monsoonal heating during summer over land. However the anticyclones thus forced are weak.
- Enhancement of the subtropical anticyclones requires air-sea interaction. Once the

subtropical anticyclones have been forced by heating over land, subsidence of dry air over the eastern subtropical oceans cools the SST while poleward advection over the western subtropical oceans warms the SST. The atmosphere is stabilized to deep convection in the east but becomes unstable in the west. The spread of deep convection from land areas to the western subtropical oceans amplifies the forcing of the atmosphere circulation and brings the subtropical anticyclones up to full strength. This is a positive feedback.

- The positive feedback is held in check by the convective cooling of the SST. More fundamentally the seasonal cycle prevents further growth as winter approaches and the western oceans are cooled by outflow of cold, dry air from the continents and both land and ocean convection retreat equatorward.
- In the Northern Hemisphere the SST asymmetry is fundamentally forced by the atmospheric circulation but its full strength requires poleward advection of warm water in the western boundary currents. However the atmosphere circulation alone is enough to create sufficient SST asymmetry that the deep convection over the ocean is placed in the west. Further enhancement of the SST asymmetry has little impact on the atmosphere circulation.
- Cloud-radiation interactions further cool the eastern subtropical oceans after other processes have already made them cool, but have little subsequent impact on the atmosphere circulation.
- In the Southern Hemisphere ocean upwelling and advection drives the seasonal cycle of the SST asymmetry but does not appear to drive the seasonal cycle of the subtropical anticyclones. However, in the idealized model presented here, and in Rodwell and Hoskins (2001), these were the most difficult of the anticyclones to model indicating that we too have not fully explained their origin.

These conclusions build on the earlier work of Rodwell and Hoskins (2001), Chen et al. (2001) and Ting (1994) by addressing the role of air sea interaction in maintaining the summer stationary waves. We have shown how the atmospheric circulation forced by monsoonal convection over land creates zonal asymmetries of SST that favor ocean

convection over the western ocean basins, providing a diabatic forcing for the atmosphere that enhances the subtropical anticyclones. While the ocean plays a crucial active role in the seasonal cycle of the subtropical anticyclones it does so primarily by mixed layer processes. Ocean heat transport *is* important in maintaining the observed strength of the SST asymmetry but has little impact on the atmosphere circulation. Convection has a threshold behavior occurring if the atmospheric column is unstable and not occurring otherwise. The atmospheric circulation influences the SST by enough to stabilize the atmosphere over the eastern basins and destabilize it over the western basins. Ocean heat transport can cool waters and surface air in the east further but since the column is already stable this will not alter the distribution of convection.

8. Appendix: Ocean mixed layer heat budget

The temperature of the mixed layer of the ocean model is determined by horizontal and vertical advection within the mixed layer and across the mixed layer base, by the net surface heat flux less the penetration of solar radiation below the mixed layer, and by vertical mixing. The temperature equation is given by:

$$\rho c_p \left(\frac{\partial T}{\partial t} + u \frac{\partial T}{\partial x} + v \frac{\partial T}{\partial y} + w \frac{\partial T}{\partial z} \right) = \frac{\partial Q}{\partial z} - \rho c_p \frac{\partial(\overline{w'T'})}{\partial z}. \quad (9)$$

Here most terms have their usual meaning, $\frac{\partial Q}{\partial z}$ is the vertical convergence of the net radiative and turbulent surface fluxes and equals the net surface heat flux (defined positive down) minus solar radiation penetration out of the bottom of the mixed layer, and $\partial\overline{w'T'}/\partial z$ is the turbulent mixing.

Integrating from the bottom of the mixed layer $z = -H$ to the surface we get:

$$\begin{aligned} \rho c_p H \frac{\partial T}{\partial t} = & -\rho c_p \left[H \left(u \frac{\partial T}{\partial x} + v \frac{\partial T}{\partial y} \right) - (T - T_H) \left(u \frac{\partial H}{\partial x} + v \frac{\partial H}{\partial y} \right) \right] - \\ & \rho c_p \left[(T - T_H) \left(\frac{\partial H}{\partial t} + w_H \right) + \overline{(w'T')}_H \right] + Q_{sfc}^{net} - Q_H^p. \end{aligned} \quad (10)$$

T_H is the temperature immediately below the mixed layer, w_H is the vertical velocity at the base of the mixed layer, Q_{sfc}^{net} is the net surface heat flux and Q_H^p is the penetrating solar radiation. The first square bracketed term is the SST tendency due to horizontal processes and the second square bracketed term is the tendency due to vertical processes. The sum of these we call the SST tendency due to ocean processes. In the Murtugudde et al. (1996) model used in the Southern Hemisphere the vertical integral is just over the bulk mixed layer while in the Lamont ocean GCM we explicitly integrate the advective terms over the levels within the mixed layer and these terms in Eq. 10 should be thought of in that way.

References

- Bergman, J. W. and H. H. Hendon: 2000, The impact of clouds on the seasonal cycle of radiative heating over the Pacific. *J. Atmos. Sci.*, **57**, 545–566.
- Betts, A. K. and W. Ridgway: 1989, Climatic equilibrium of the atmospheric convective boundary layer over a tropical ocean. *J. Atmos. Sci.*, **46**, 2621–2641.
- Bishop, J. K. B. and W. B. Rossow: 1991, Spatial and temporal variability of global surface solar irradiance. *J. Geophys. Res.*, **96**, 16 839–16 858.
- Blumenthal, M. B.: 1990, Effects of West African air humidity on Atlantic sea surface temperature. *Greenhouse Effect, Sea Level and Drought*, P. R. Paepe, R. W. Fairbridge, and S. Jelgersma, eds., Kluwer Academic Publishers, Dordrecht, The Netherlands, NATO Advanced Research Workshop on Geohydrological Management of Sea Level and Mitigation of Drought, 21–40.
- Chen, D., L. M. Rothstein, and A. J. Busalacchi: 1994, A hybrid vertical mixing scheme and its application to tropical ocean models. *J. Phys. Oceanogr.*, **24**, 2156–2179.
- Chen, P., M. P. Hoerling, and R. M. Dole: 2001, The origin of the subtropical anticyclones. *J. Atmos. Sci.*, **58**, 1827–1835.
- daSilva, A., A. C. Young, and S. Levitus: 1994, Atlas of surface marine data 1994. Volume 1. Algorithms and Procedures. Technical Report NOAA SMD94, National Oceanographic and Atmospheric Administration, Washington, DC, 83pp.
- Del Genio, A. D., M.-Y. Yao, W. Kovari, and K. K.-W. Lo: 1996, A prognostic cloud water parameterization for global climate models. *J. Climate*, **9**, 270–304.
- Gent, P. and M. A. Cane: 1989, A reduced gravity, primitive equation model of the upper equatorial ocean. *J. Comp. Phys.*, **81**, 444–480.
- Hansen, J. E., A. Lacis, D. Rind, G. Russel, P. Stone, I. Fung, R. Ruedy, and J. Lerner: 1984, Climate sensitivity: Analysis of feedback mechanisms. *In: Climate processes and climate sensitivity. Geophys. Mongr. Ser. 29*, J. E. Hansen and T. Takahashi, eds., American Geophysical Union, Washington DC, 130–163.

- Hartmann, D. L., M. E. Ockert-Bell, and M. Michelsen: 1992, The effect of cloud type on Earth's energy balance: Global analysis. *J. Climate*, **5**, 1281–1304.
- Held, I. and M. Suarez: 1994, A proposal for the intercomparison of the dynamical cores of atmospheric general circulation models. *Bull. Amer. Meteor. Soc.*, **75**, 1825–1830.
- Kalnay, E. et al.: 1996, The NCEP/NCAR 40-year reanalysis project. *Bull. Am. Meteor. Soc.*, **77**, 437–471.
- Kiehl, J. T., J. J. Hack, G. B. Bonan, B. A. Bovile, D. L. Williamson, and P. J. Rasch: 1998, The National Center for Atmospheric Research Community Climate Model: CCM3. *J. Climate*, **11**, 1131–1149.
- Kistler, R. et al.: 2001, The NCEP-NCAR 50-year Reanalysis: Monthly means CD-ROM and documentation. *Bull. Am. Meteor. Soc.*, **82**, 247–268.
- Klein, S. A. and D. L. Hartmann: 1993, The seasonal cycle of low stratiform clouds. *J. Climate*, **6**, 1587–1606.
- Li, Z. and H. G. Leighton: 1993, Global climatologies of the solar radiation budgets at the surface and in the atmosphere from 5 years of ERBE data. *J. Geophys. Res.*, **98**, 4919–4930.
- Murtugudde, R., R. Seager, and A. J. Busalacchi: 1996, Simulation of the tropical oceans with an ocean GCM coupled to an atmospheric mixed layer model. *J. Climate*, **9**, 1795–1815.
- Philander, S., D. Gu, D. Halpern, N. Lau, T. Li, and R. Pacanowski: 1996, Why the ITCZ is mostly north of the equator. *J. Climate*, **9**.
- Rodwell, M. J. and B. J. Hoskins: 2001, Subtropical anticyclones and summer monsoons. *J. Climate*, **14**, 3192–3211.
- Russell, G. L., J. R. Miller, and L.-C. Tsang: 1985, Seasonal oceanic heat transports computed from an atmospheric model. *Dyn. Atmos. Oceans*, **9**, 253–271.

- Seager, R., D. Battisti, J. Yin, N. Naik, N. Gordon, A. Clement, and M. A. Cane: 2002, Is the Gulf Stream responsible for Europe's mild winters? *Quart. J. Royal Meteor. Soc.*, in press.
- Seager, R. and M. B. Blumenthal: 1994, Modeling tropical Pacific sea surface temperature with satellite-derived solar radiative forcing. *J. Climate*, **7**, 1943–1957.
- Seager, R., M. B. Blumenthal, and Y. Kushnir: 1995, An advective atmospheric mixed layer model for ocean modeling purposes: Global simulation of surface heat fluxes. *J. Climate*, **8**, 1951–1964.
- Seager, R., Y. Kushnir, N. Naik, M. A. Cane, and J. Miller: 2001, Wind-driven shifts in the latitude of the Kuroshio-Oyashio extension and generation of SST anomalies on decadal timescales. *J. Climate*, **14**, 4249–4265.
- Seager, R., Y. Kushnir, M. Visbeck, N. Naik, J. Miller, G. Krahnemann, and H. Cullen: 2000, Causes of Atlantic Ocean climate variability between 1958 and 1998. *J. Climate*, **13**, 2845–2862.
- Ting, M.: 1994, Maintenance of northern summer stationary waves in a GCM. *J. Atmos. Sci.*, **51**, 3286–3308.
- Visbeck, M., H. Cullen, G. Krahnemann, and N. Naik: 1998, An ocean model's response to North Atlantic Oscillation-like wind forcing. *Geophys. Res. Letters*, **25**, 4521–4524.
- Xie, P. and P. A. Arkin: 1996, Analyses of global monthly precipitation using gauge observations, satellite estimates, and numerical model predictions. *J. Climate*, **9**, 840–858.

List of Figures

1	Sea level pressure (mb), surface winds and the departure from the zonal mean of sea surface temperature ($^{\circ}C$) for (a) December, January and February, (b) March, April and May, (c) June, July and August and (d) September, October and November from NCEP-NCAR Reanalysis.	30
2	Precipitation (mm/day) and subsidence (Pa/s) for (a) December, January and February, (b) March, April and May, (c) June, July and August and (d) September, October and November. The precipitation is from Xie and Arkin (1996) and the subsidence is from NCEP-NCAR Reanalysis.	31
3	The moist static instability, defined as the moist static energy at 1000mb minus the saturation moist static energy at 700mb for (a) December, January and February, (b) March, April and May, (c) June, July and August and (d) September, October and November. The data are from NCEP-NCAR Reanalysis. Units are $10^3 J/kg$	32
4	(a) the mean advection of moist static energy, (b) transient moist static energy flux divergence, (c) the sum of ocean advection and mixing and (d) the net surface solar radiation for December, January and February. The advection and transient flux divergence are evaluated from NCEP-NCAR Reanalysis, the ocean processes tendency from the ocean GCM and the net surface solar radiation from ERBE. All terms are plotted as positive if they tend to increase the SST and are in Wm^{-2}	33
5	Same as Figure 4 but for June, July and August	34

6	Time-longitude plots of the (a) the SST, (b) the mean moist static energy advection, (c) the transient eddy flux divergence of moist static energy, (d) the net surface radiation, (e) the sum of ocean advection and mixing and (f) the sum of boundary layer radiative cooling and turbulent flux of moist static energy at $700mb$ for the North Pacific. Data are averaged from $15^\circ - 35^\circ N$ and are plotted as the departure from the zonal average across the basin. Positive values indicate a warming. Data are from NCEP-NCAR Reanalyses except the surface solar which is from ISCCP and the ocean advection and mixing which are from the ocean GCM. Units are K for (a) and otherwise Wm^{-2}	35
7	The same as Figure 6 but for the North Atlantic.	36
8	The same as Figure 6 but for the South Pacific.	37
9	The same as Figure 6 but for the South Atlantic.	38
10	The deviation of SST from zonal symmetry and the sea level pressure from the experiment with the GISS atmospheric GCM coupled to a mixed layer ocean. (a) DJF with q-flux, (b) DJF without q-flux, (c) JJA with q-flux and (d) JJA without q-flux.	39
11	Same as Figure 10 but from the CCM3 atmospheric GCM coupled to a mixed layer ocean.	40
12	(a) The sea level pressure and SST asymmetry in the idealized model forced by observed condensational heating over, (a) land (contour interval $2mb$) (b) land plus the equatorial ocean (contour interval $2mb$) and (c) all land and all ocean (contour interval $5mb$) for December through February. . . .	41
13	Same as Figure 12 except for June through August.	42

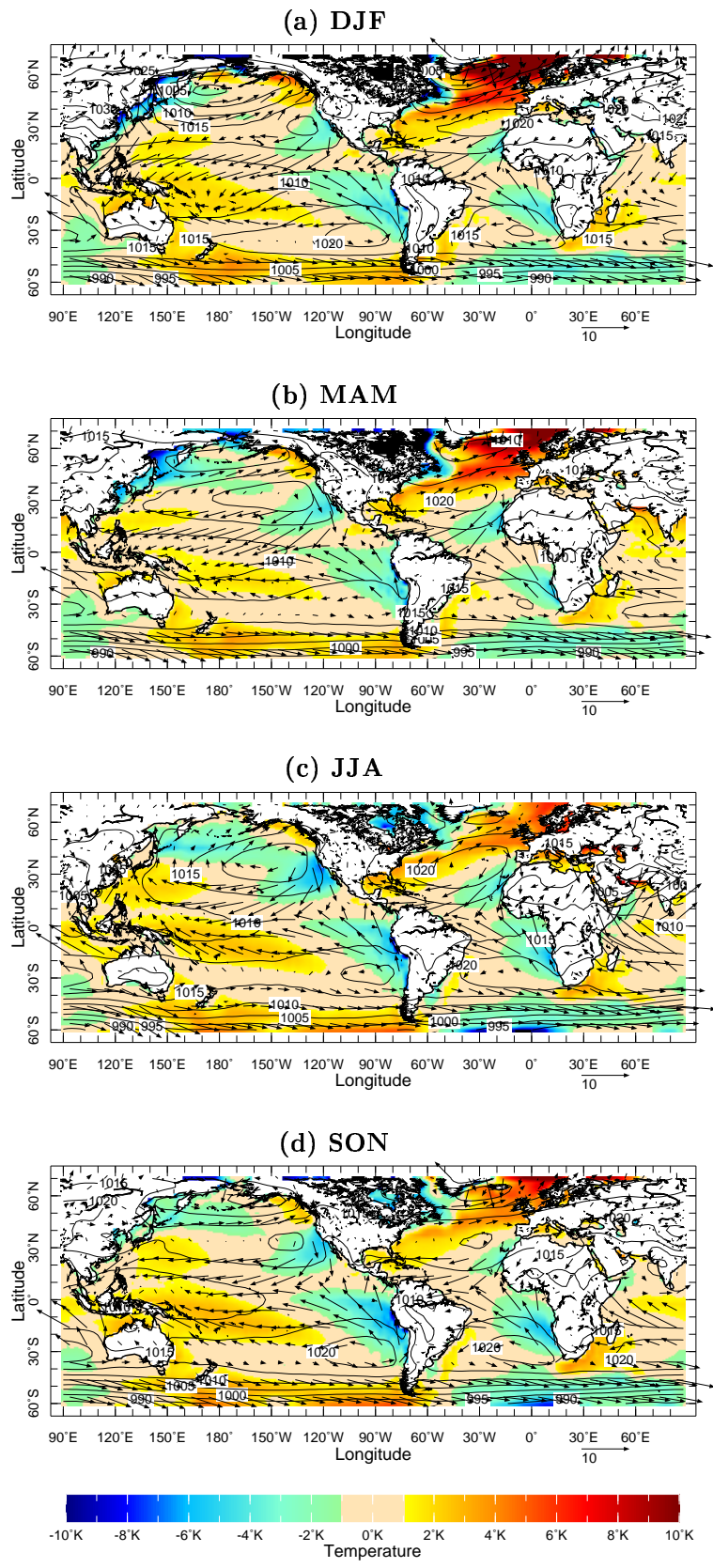


Figure 1: Sea level pressure (mb), surface winds and the departure from the zonal mean of sea surface temperature ($^{\circ}C$) for (a) December, January and February, (b) March, April and May, (c) June, July and August and (d) September, October and November from NCEP-NCAR Reanalysis.

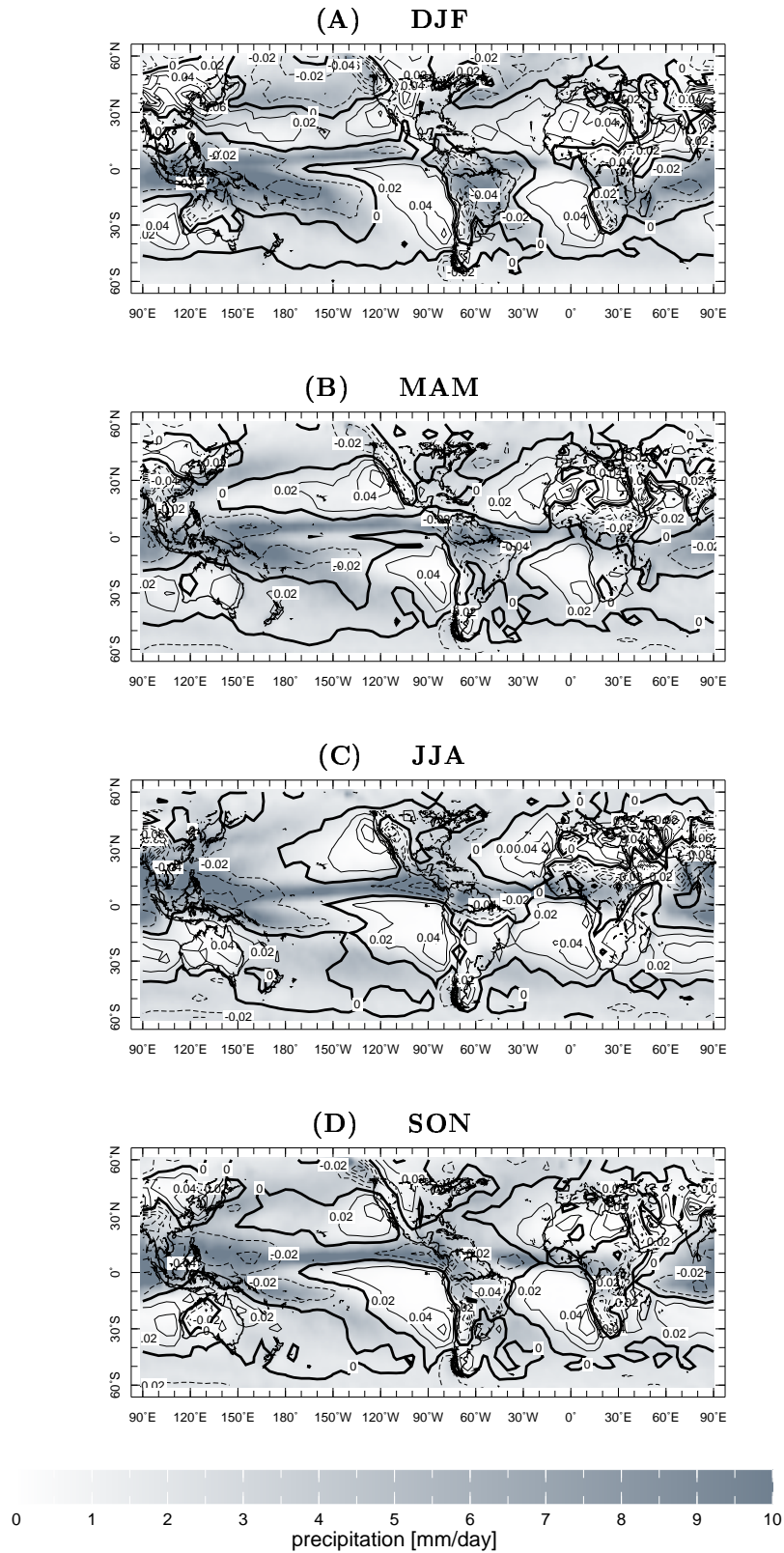


Figure 2: Precipitation (mm/day) and subsidence (Pa/s) for (a) December, January and February, (b) March, April and May, (c) June, July and August and (d) September, October and November. The precipitation is from Xie and Arkin (1996) and the subsidence is from NCEP-NCAR Reanalysis.

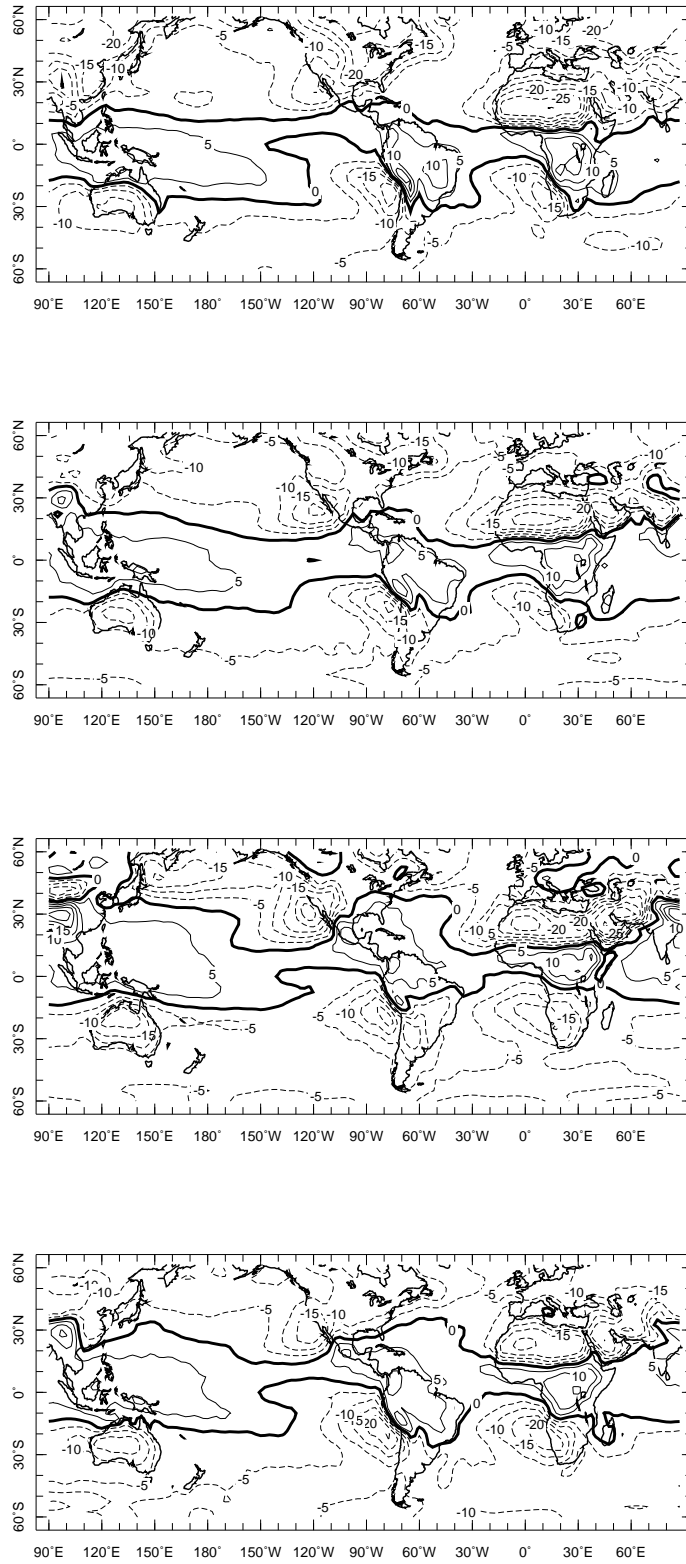


Figure 3: The moist static instability, defined as the moist static energy at 1000mb minus the saturation moist static energy at 700mb for (a) December, January and February, (b) March, April and May, (c) June, July and August and (d) September, October and November. The data are from NCEP-NCAR Reanalysis. Units are $10^3 J/kg$

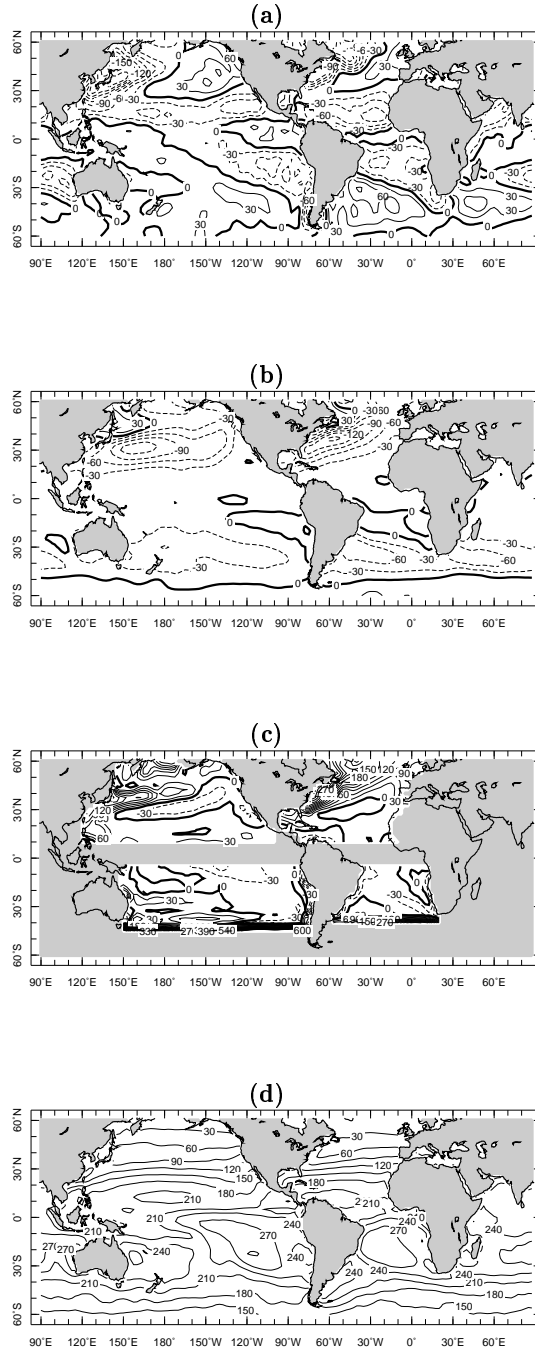


Figure 4: (a) the mean advection of moist static energy, (b) transient moist static energy flux divergence, (c) the sum of ocean advection and mixing and (d) the net surface solar radiation for December, January and February. The advection and transient flux divergence are evaluated from NCEP-NCAR Reanalysis, the ocean processes tendency from the ocean GCM and the net surface solar radiation from ERBE. All terms are plotted as positive if they tend to increase the SST and are in Wm^{-2} .

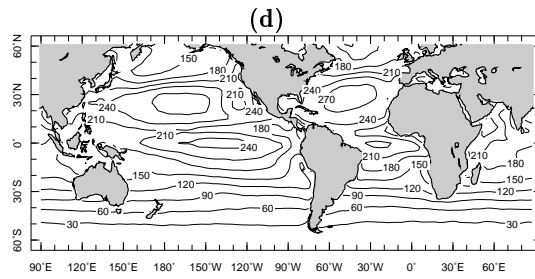
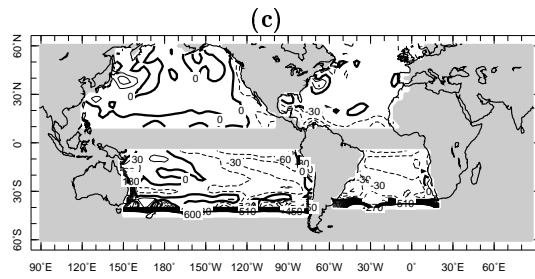
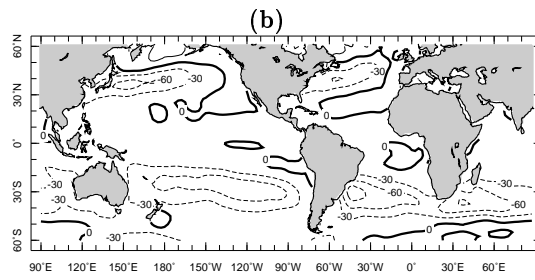
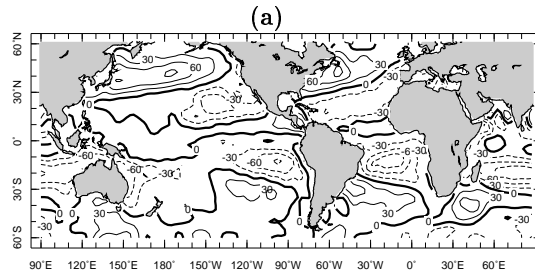


Figure 5: Same as Figure 4 but for June, July and August

fig:5

Observed North Pacific (15N to 35N) Deviation from basin mean

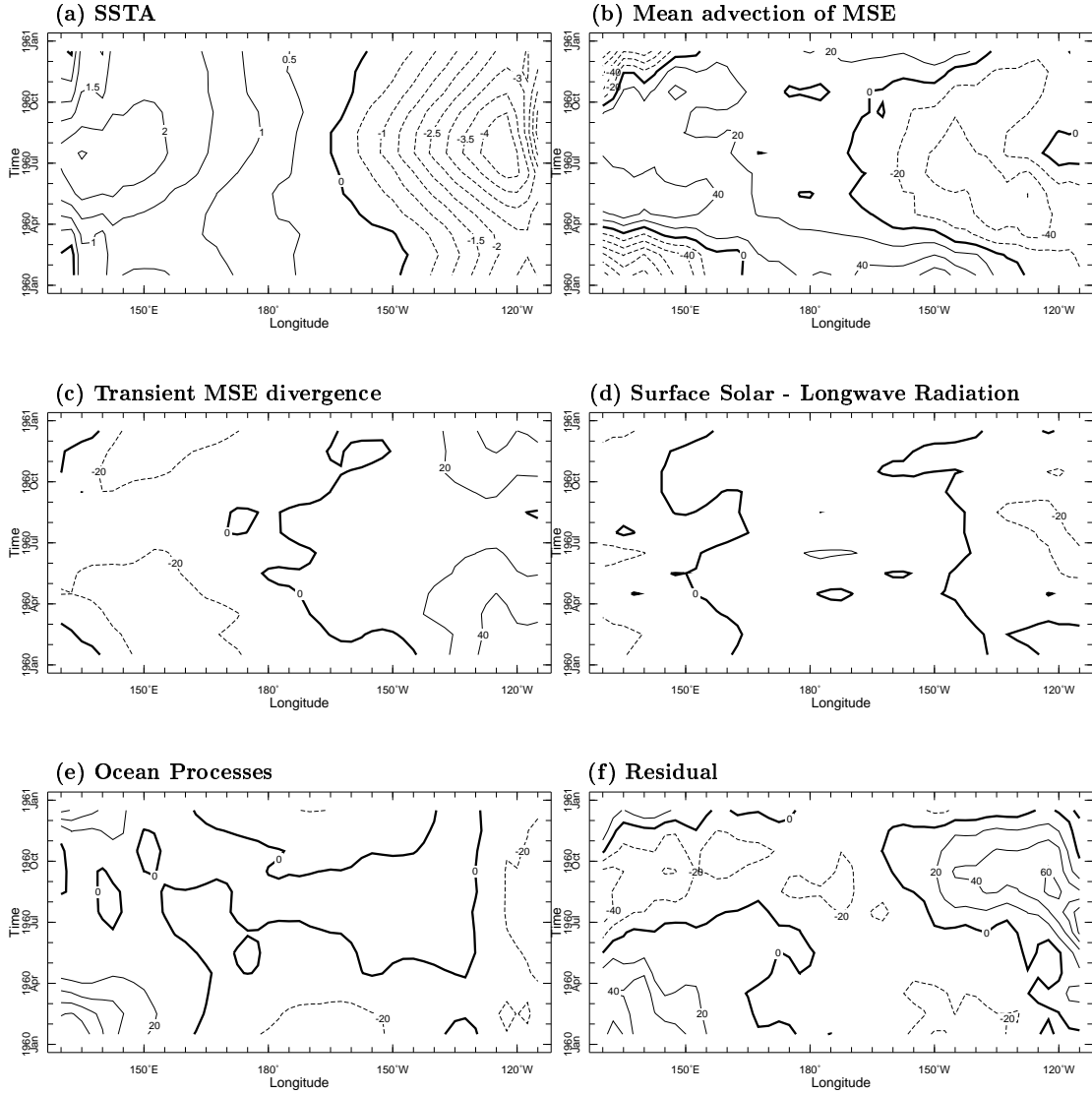


Figure 6: Time-longitude plots of the (a) the SST, (b) the mean moist static energy advection, (c) the transient eddy flux divergence of moist static energy, (d) the net surface radiation, (e) the sum of ocean advection and mixing and (f) the sum of boundary layer radiative cooling and turbulent flux of moist static energy at 700mb for the North Pacific. Data are averaged from 15° – 35°N and are plotted as the departure from the zonal average across the basin. Positive values indicate a warming. Data are from NCEP-NCAR Reanalyses except the surface solar which is from ISCCP and the ocean advection and mixing which are from the ocean GCM. Units are K for (a) and otherwise Wm^{-2} .

fig:6

Observed North Atlantic (15N to 35N) Deviation from basin mean

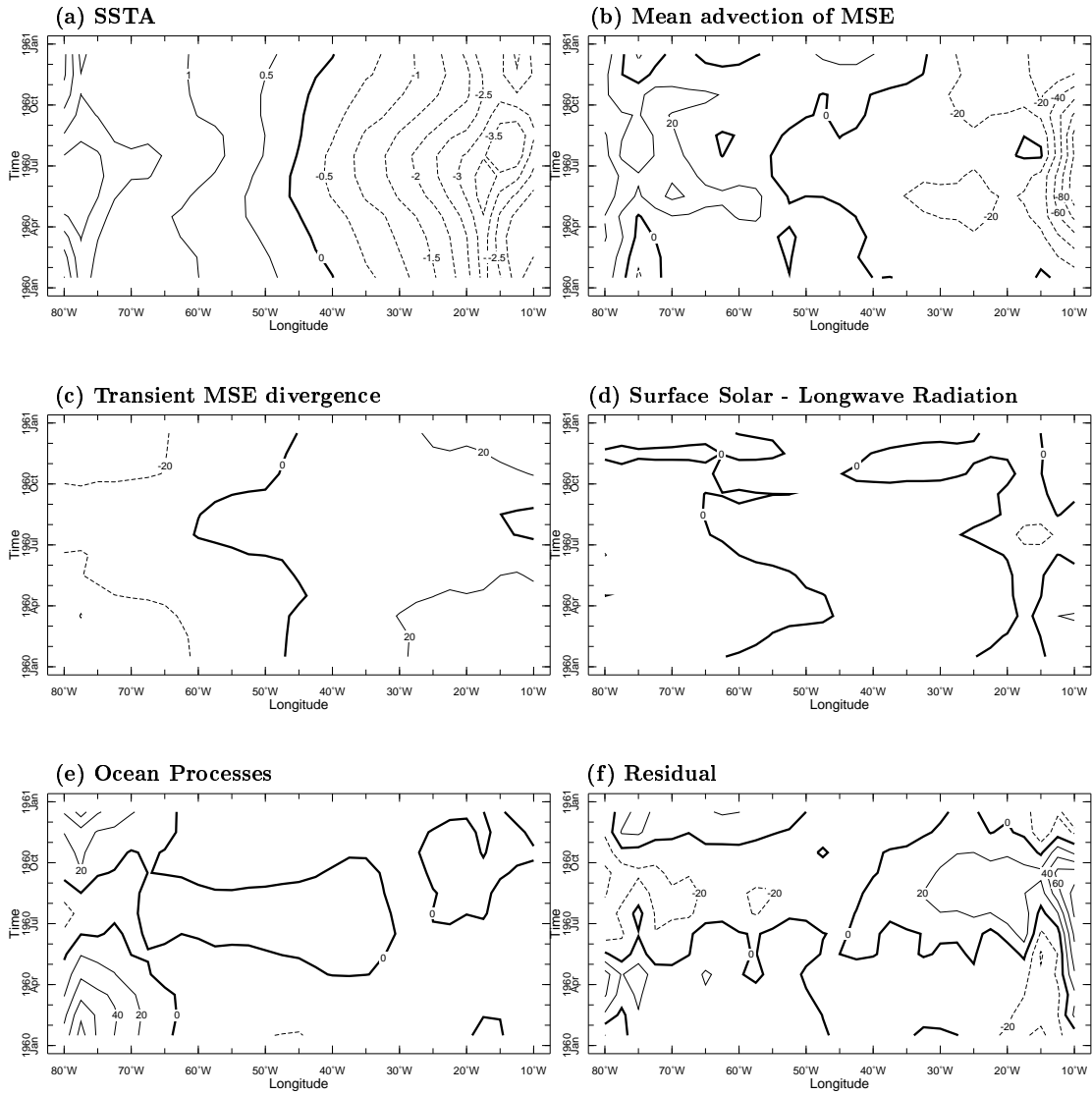


Figure 7: The same as Figure 6 but for the North Atlantic.

fig:7

Observed South Pacific (5S to 25S) Deviation from basin mean

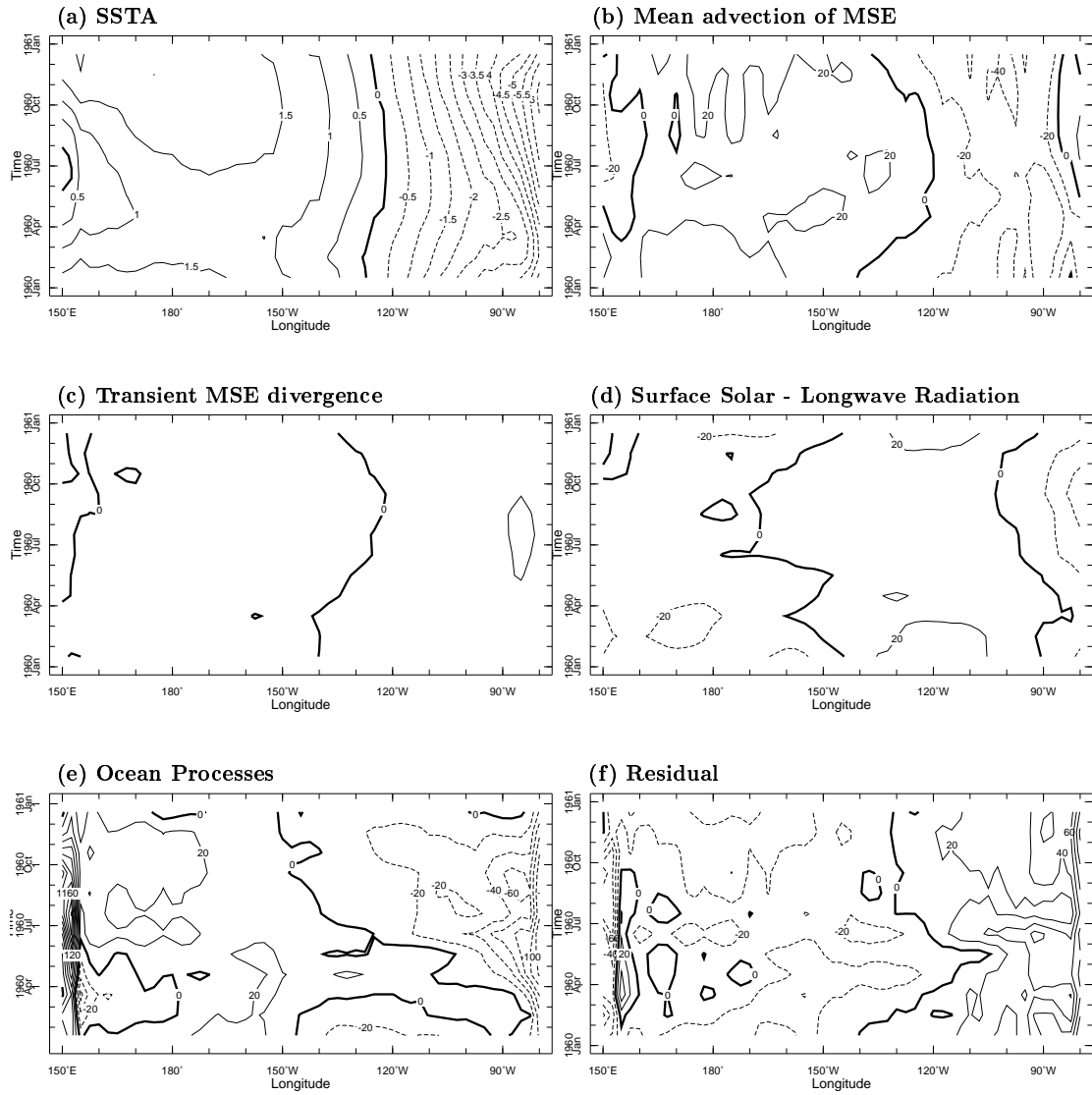


Figure 8: The same as Figure 6 but for the South Pacific.

fig:8

Observed South Atlantic (5S to 25S) Deviation from basin mean

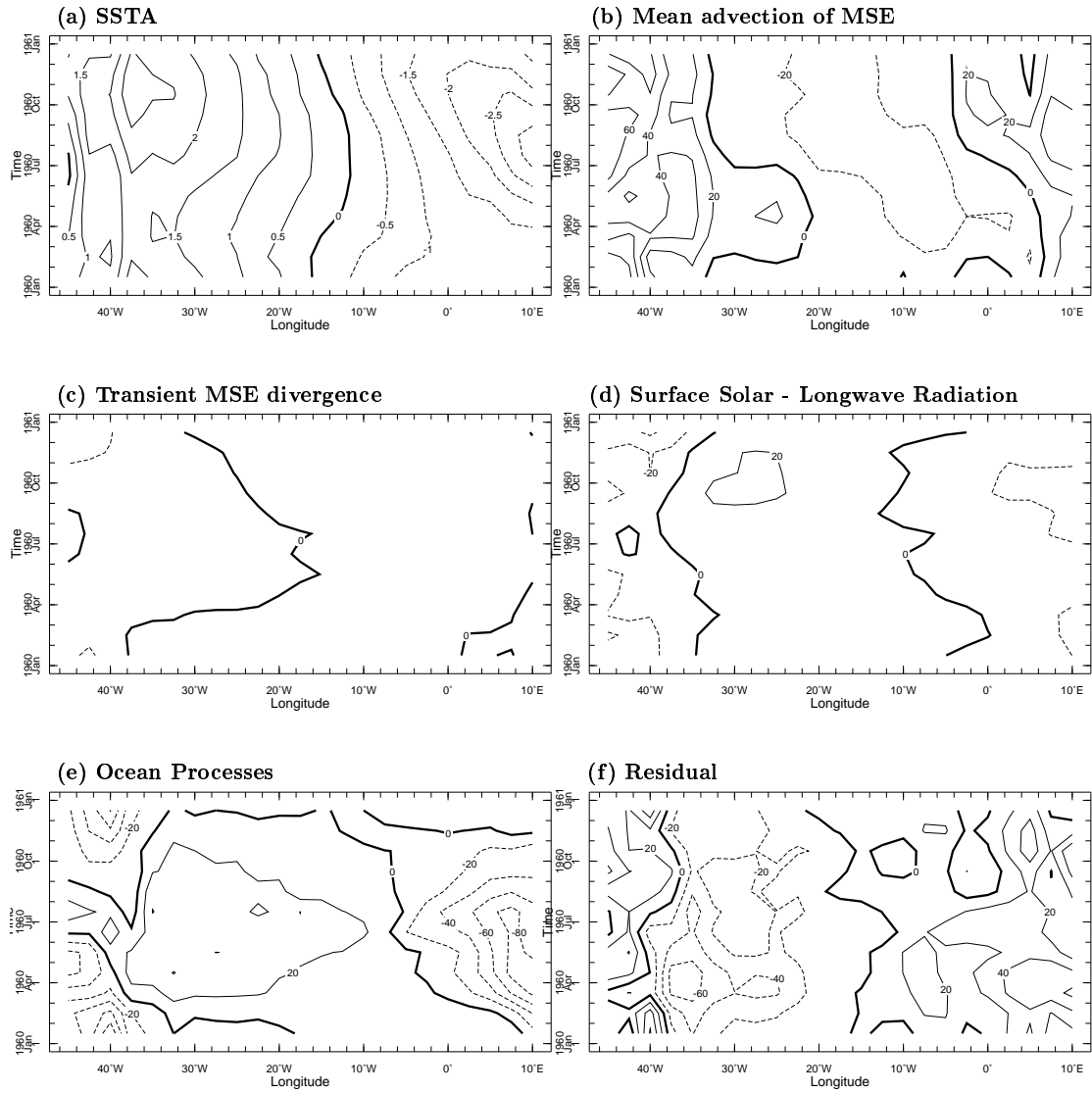


Figure 9: The same as Figure 6 but for the South Atlantic.

fig:9

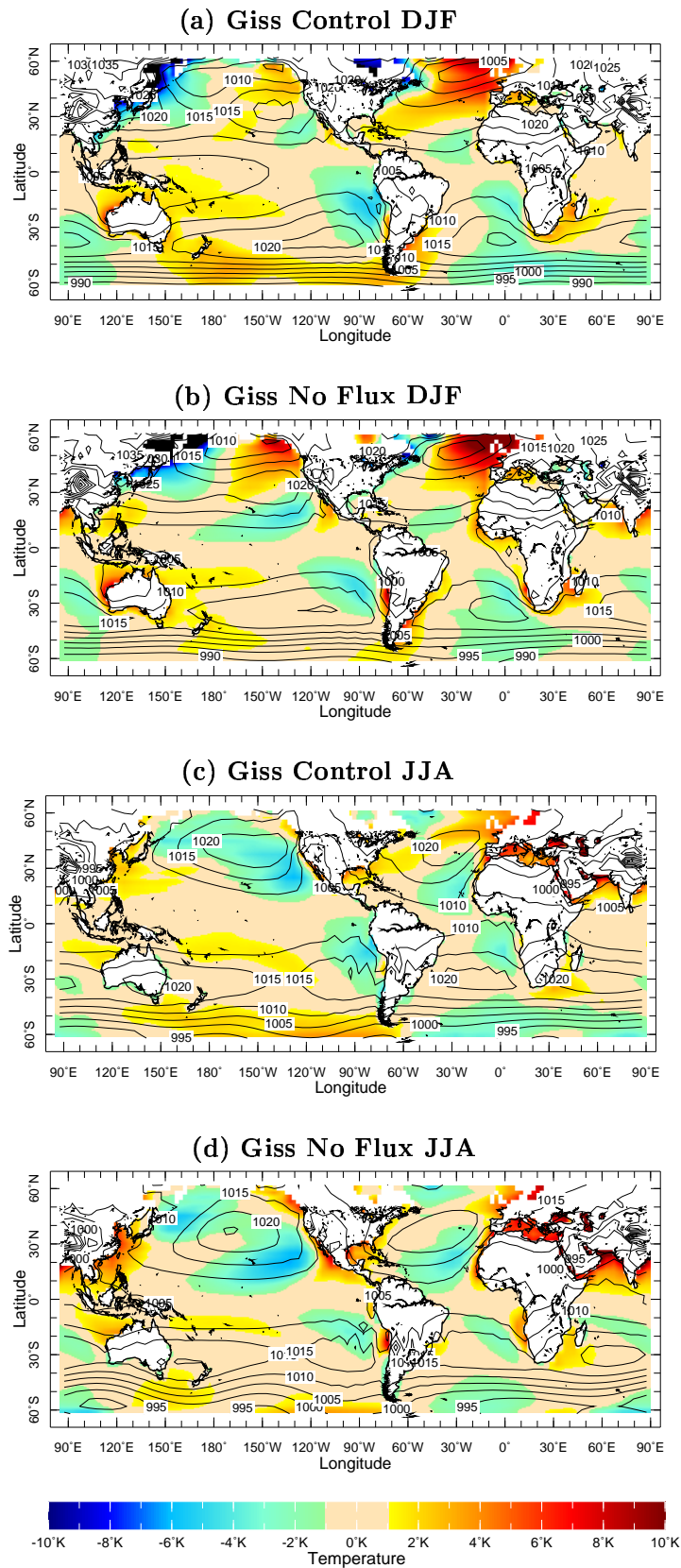


Figure 10: The deviation of SST from zonal symmetry and the sea level pressure from the experiment with the GISS atmospheric GCM coupled to a mixed layer ocean. (a) DJF with q-flux, (b) DJF without q-flux, (c) JJA with q-flux and (d) JJA without q-flux.

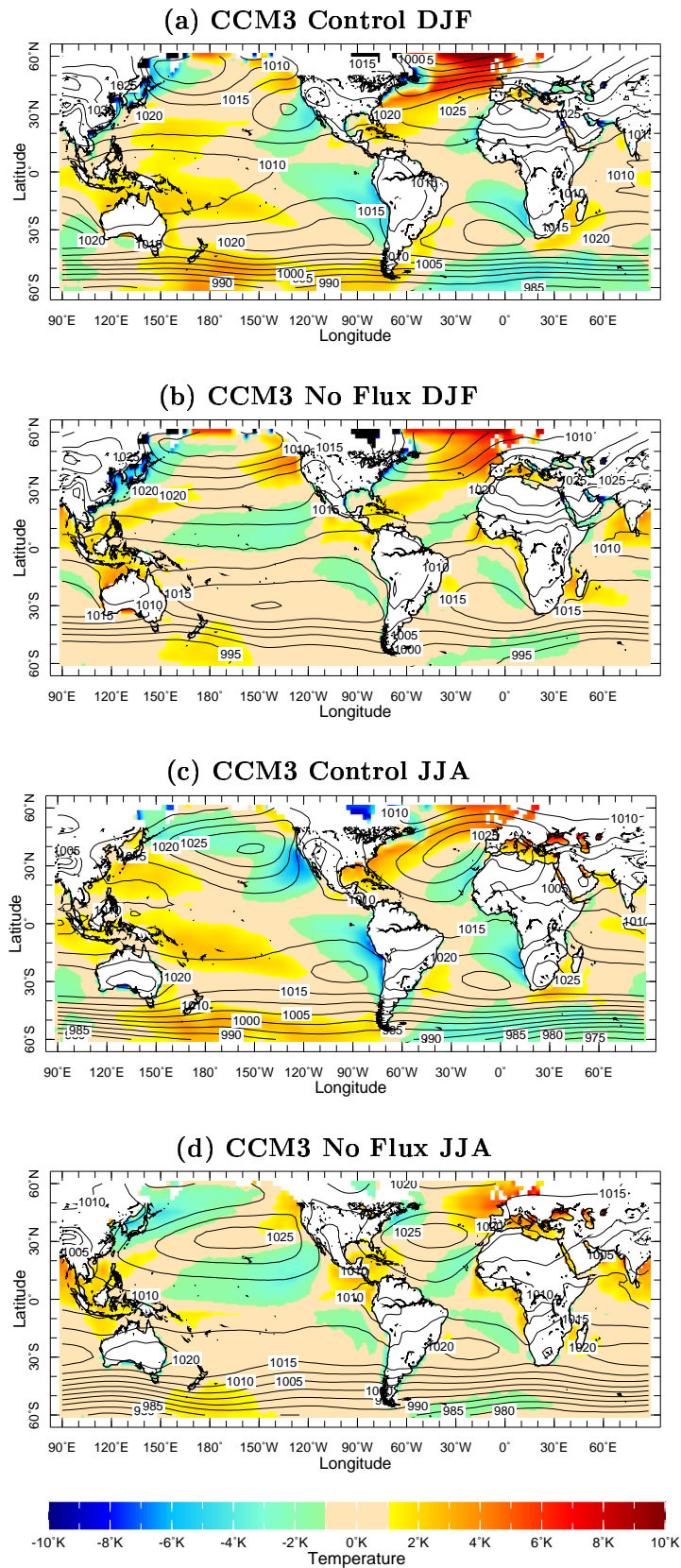


Figure 11: Same as Figure 10 but from the CCM3 atmospheric GCM coupled to a mixed layer ocean.

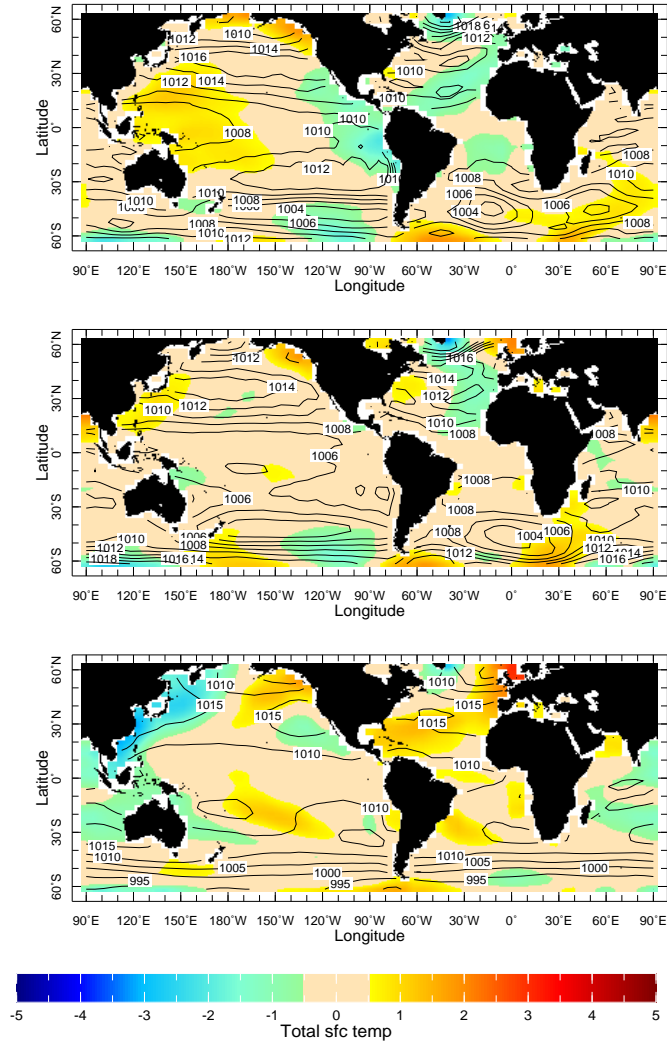


Figure 12: (a) The sea level pressure and SST asymmetry in the idealized model forced by observed condensational heating over, (a) land (contour interval $2mb$) (b) land plus the equatorial ocean (contour interval $2mb$) and (c) all land and all ocean (contour interval $5mb$) for December through February.

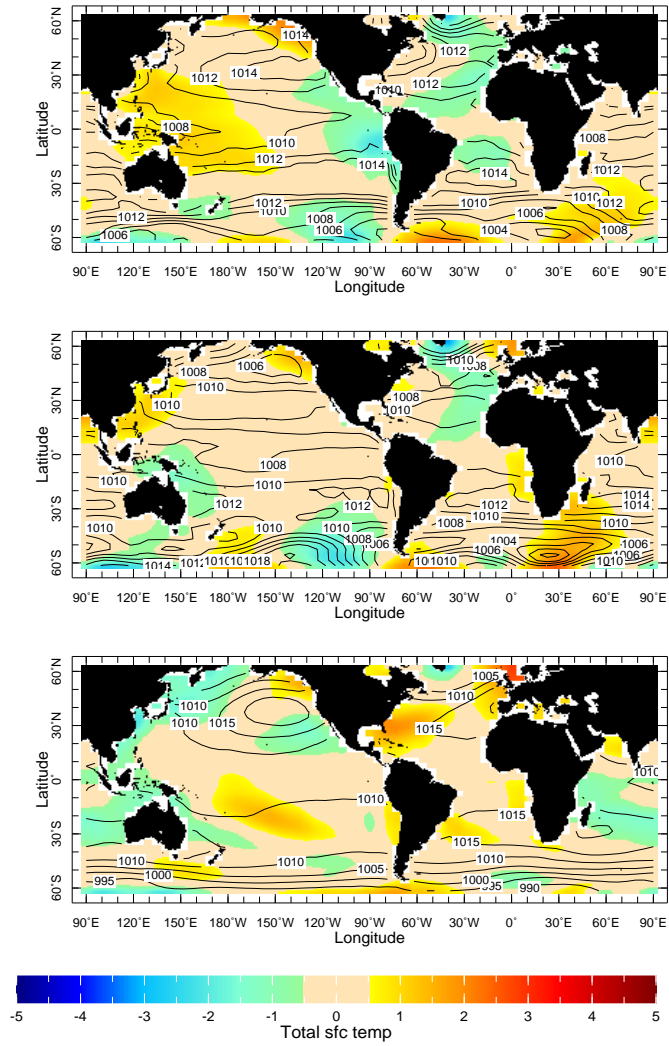


Figure 13: Same as Figure 12 except for June through August.